Influence of pressure on the change of temperature inside the elastic element under dynamic stress

Jozef Krajňák[0000-0003-3497-3639], *Robert* Grega[0000-0003-4649-1274], and *Michal* Puškár[0000-0001-6042-8779]

Department of KaDI, Faculty of Mechanical Engineering, Technical University of Košice, Letná 9, 04001 Košice, Slovakia

Abstract. The article describes the change in temperature inside the elastic element when the pressure changes. These flexible elements are used in flexible pneumatic couplings developed at our workplace and are pressurized by a certain value of pressure depending on the transmitted torque. We test the given elements on a test rig designed at our workplace. It describes this device in detail in this article. On this device we test these elastic elements at different pressures. We find out how much influence the pressure value in the elastic element has on the change of temperature inside the element. We will find out whether the change in pressure also has a significant effect on the change in temperature and whether this temperature also affects the functionality of the device in which these elements are used.

1 Introduction

When designing torsionally oscillating mechanical systems, it is necessary to proceed in such a way that the adverse effects of torsional vibrations are eliminated as much as possible [15], [20]. At our workplace, we have been dealing with this issue for a long time, which is also related to the transmission of torque. During the transmission of torque, vibrations, torsional vibrations and noise arise [4,] [8], [10]. Therefore, it is important to prevent such mechanisms in some way so as not to damage some members or possibly damage the entire device [11], [12], [14]. To reduce the adverse effects of torsional vibrations, it is advantageous to use flexible shaft couplings. These make it possible to tune the torsionally oscillating system and adjust its stiffness, damping or mass parameters so that its dangerous resonant state does not occur during the operating mode of the system [18], [19], [27]. In the field of tuning torsionally oscillating mechanical systems, high-elastic shaft couplings are currently used at our workplace. High-spring linear or non-linear shaft couplings are currently used in the field of tuning torsionally oscillating mechanical systems. [1], [2], [3].

These shaft couplings use flexible elements to transfer energy. These resilient elements are dynamically stressed and heat is generated as a result of this stress. These resilient elements are manufactured by different manufacturers with different mixtures of rubbers or complementary other materials. Rubber as a material is quite sensitive to heat, it is

important to find out what temperatures arise during operation in these elements and whether this temperature does not exceed the safe temperatures specified by the manufacturer. An increase in temperature can cause a change in the properties of the rubber and thus a change in the properties of the entire mechanical system in which they are used. The temperature of the elastic members affects the modulus of elasticity of the rubber in compression, the damping, relaxation, aging and fatigue of the rubber. We want to avoid this change because it is disadvantageous for us and is a potential source of failure for the entire device.
At the Department of Structural and Transport Engineering of the FME TU in Košice, attention has been paid for a long time to the development and research of pneumatic flexible shaft couplings [9], [16], [7].
The aim of the article is to find out how the temperature inside the elastic element will change at different pressures in the elastic element during the dynamic stressing of this member.

2 Examined elastic elements

The There are various manufacturers of flexible elements in the world. Different sizes and different numbers of bellows are also produced. Most single-wave, double-wave and triple-wave elements are produced Fig. 1. Different manufacturers offer different shapes of flanges to hold the flexible element. The air supply is usually routed through the center and the flange is anchored with four screws. The most commonly used single-wavy and double-wavy elastic elements of Fig. 1b. but in cases that we need to achieve a larger stroke or compression, we can also use a three-wave element Fig. 1a.

Fig. 1. Types of flexible pneumatic elements.

These flexible elements are friction-free and require maintenance and lubrication. They are designed for low strokes and high pressures. The height of the pneumatic element depends on the diameter of the cylinder and the number of bellows. The higher the height of the element, the larger the dimensions of the pneumatic shaft coupling in which this element is mounted.

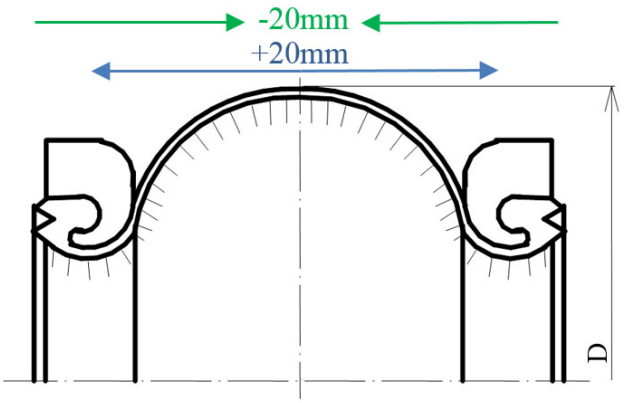

Fig. 2. Investigated flexible pneumatic element PE 130/1.

The construction provides insulation against shocks and manufacturers also offer various types of anchoring flanges, which ensures easy assembly of the element. The working pressure is limited by the maximum working pressure which is 800kPa.Normal operating temperature is in the range of -40 °C to 70 °C. For special operations, the manufacturer can provide another material that has a working temperature in the range of -20 °C to 115 °C.
For our research, we used a flexible pneumatic element PE 130/1. The marking itself defines the diameter of the cylinder D = 130mm and the number of bellows (Fig.2). We used a single-wavy element for our research. The temperature changes during the compression of the single-wave double-wave and triple-wave elements are very similar.

3 Description of the test equipment

We performed all measurements on a test rig located in the laboratory of our department. A diagram of a test device for measuring the temperatures of a separate pneumatic-elastic elementPE-130/1 is shown in Fig. 3. This device allows us to stress the elastic elements by dynamic stress at different speeds, and we can also change the amplitude of the stress in a certain range.

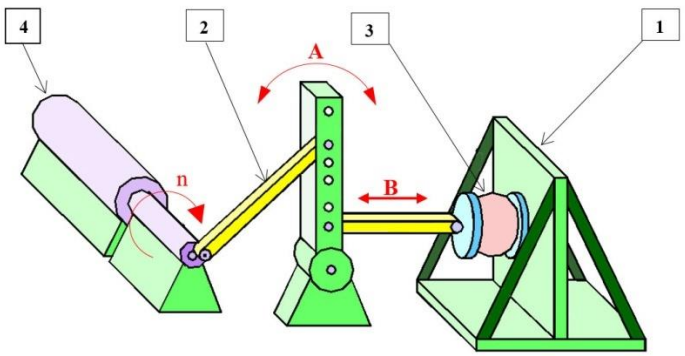

Fig. 3. The scheme of the test apparatus for measuring the temperature.

The test device consists of a disassembly of the frame (1), in which the pneumatic-elastic element PE-130/2 (3) is mounted. This element is double-wavy and we use it in flexible pneumatic shaft couplings developed at our department. These elements are made of rubber cord material and can operate at a working pressure of 100-700kPa. The converter of rotary motion to rectilinear reciprocating motion (2) was also developed at our department and by simply changing the arm mounting we can change the amplitude of dynamic stress. To drive the entire device, we use a DC electric motor (4) type SM 160L with an output of 16 kW with an additional thyristor speed controller type IRO with the possibility of a smooth change of speed from 0 - 2000 min^{-1}.
The electric motor can rotate in the range of 0 - 2000 min^{-1}. We performed our measurements at three different speeds n = 400min^{-1}, n = 600min^{-1} and n = 800min^{-1}.
Due to the rotation of the electric motor, the proposed mechanism consisting of two arms and one lever (2) performs an oscillating movement A. The speed of this oscillating movement depends on the speed and the amplitude of the oscillation depends on the grip of the arm (2). As a result of the oscillating movement, the flexible pneumatic element (3) performs a rectilinear reciprocating movement B. The measurements were performed at amplitude A = 5.6 mm. By changing the mounting of the arm (3), we can change the amplitude of the breaks. M-3870D METEX touch digital multimeters with ETP-003 thermal probe: -50 - +250 °C were used to examine the temperature. Using them, we monitored the temperature of its inner surface T_{in}.The ambient temperature was T_0 = 22 °C at the beginning of the measurement. The stated temperatures were recorded at times t = 1, 2, 3, 4, 5, ... 29, 30 min at the set speeds, air pressure and deformation amplitude.

4 Results of experimental measurements

We performed all measurements on the test equipment Fig. 3. The course of the measured values can be seen in Fig.4, Fig. 5 and Fig. 6.
We performed measurements successively at pressures of 0kPa, 200kPa, 300kPa, 500kPa and 600kPa and speeds of 400min^{-1}, 600min^{-1} and 800min^{-1}. Temperatures of the inner surface of the elastic element were recorded using a sensor at 0 to 30 minutes. We recorded the values every minute. After several measurements, we found that after 25 minutes, the temperature mostly stabilized. After 30 minutes, the temperature no longer changed and the courses were constant.
The temperature of the inner surface T_{in} of the elastic element at the set amplitude A = 5.6 mm and speed n = 400 min^{-1} varied in the range of 22.5 °C to 26 °C. At a pressure of 0 kPa, the value increased to25 °C and remained constant. The temperature of the inner surface of the surface of the elastic element at a pressure p = 200 kPa varied in the same way as at a pressure p = 0 kPa in the range 22.5 °C to25 °C. The temperature of the inner surface of the elastic element at a pressure p = 300 kPa acquired slightly higher values than at a pressure p = 0 kPa in the range 22.5 °C to 26 °C. The temperature of the inner surface of the elastic element at a pressure p = 500kPa varied in the same way as at a pressure p = 0kPa and p = 200kPa in the range 22.5 ° C to 25 °C. At a pressure of p = 600 kPa, the temperature of the inner surface reached the lowest rise and only in the range of 22.5 °C to 24 °C. We can state that at speed n = 400min-1 it did not change much on a large scale and had rather a small tendency to decrease with increasing value of pressure.

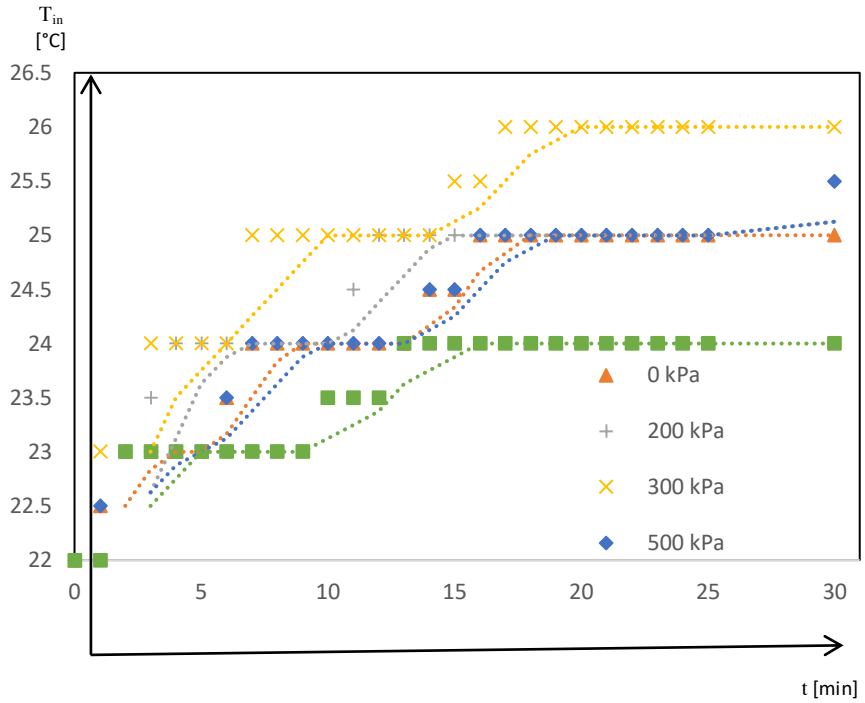

Fig. 4. The course of the temperature T_{in} at different pressures and speeds 400min^{-1}.

The temperature of the inner surface Tin of the elastic element at the set amplitude A = 5.6 mm and speed n = 600 min^{-1} varied in the range of 22.5 °C to 27 °C. At a pressure of 0 kPa, the value increased to 26 °C and remained constant. The temperature of the inner surface of the surface of the elastic element Tin at a pressure p = 200 kPa reached the highest value and varied in the range of 22.5 °C to 27.5 °C. The temperature of the inner surface of the elastic element at a pressure p = 300kPa acquired similar values as at a pressure p = 200kPa in the range 22.5 °C to 27 °C. The temperature of the inner surface of the elastic element at a pressure p = 500kPa reached a lower value than at a pressure p = 200kPa and p = 300kPa in the range 22.5 °C to 26 °C. At a pressure of p = 600 kPa, the temperature of the inner surface reached the lowest rise and only in the range of 22.5 °C to 25 °C. We can state that at speed n = 600min^{-1} the course of temperatures was similar to that at speed n = 400min^{-1}.The course of temperatures also tended to decrease with increasing pressure value.

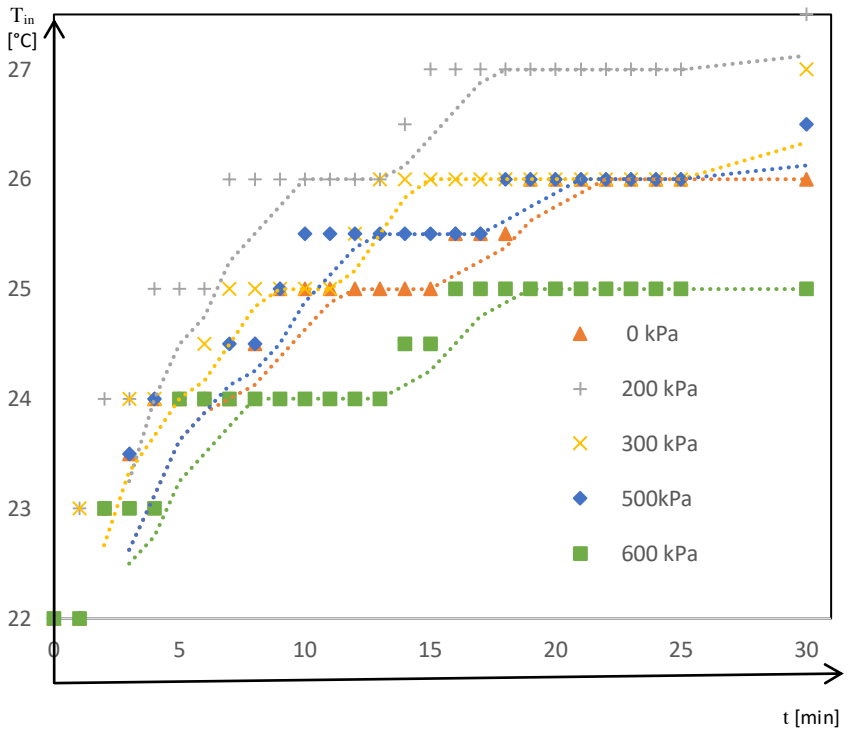

Fig. 5. The course of the temperature T_{in} at different pressures and speeds 600min^{-1}.

In the next Fig. 6 we can observe the course of the temperature of the inner surface Tin of the elastic element at the set amplitude A = 5.6 mm and the speed n = 800 min^{-1} varied in the range of 22.5 °C to 29 °C. At a pressure of 0 kPa, the value increased to 28 °C and remained constant. The temperature of the inner surface of the surface of the elastic element T_{in} at a pressure p = 200 kPa reached the highest value and varied in the range of 22.5 °C to 29 °C. The temperature of the inner surface of the elastic element at a pressure p = 300kPa acquired lower values than at a pressure p = 200kPa in the range 22.5 °C to 28 °C. The temperature of the inner surface of the elastic element at a pressure p = 500kPa reached an even lower value than at a pressure p = 200kPa and p = 300kPa in the range 22.5 °C to 27 °C. At a pressure of p = 600 kPa, the temperature of the inner surface reached the lowest rise and only in the range of 22.5 °C to 25.5 °C. We can state that at speed n = 600min^{-1} the course of temperatures showed the highest influence of pressure on the change of temperature. The course was similar to the speed n = 400min^{-1} and n = 600min^{-1}. We can state interestingly the finding that with increasing pressure the temperature of the inner surface tends to decrease.

Interesting waveforms are shown in Fig. 4, Fig. 5 and Fig. 6. On the given waveforms we can observe the change of the temperature of the inner surface Tin at different values of pressure (0, 200, 300, 500 and 600 kPa) and different frequencies of periodic deformations 400, 600 and 800 min^{-1}. Here we see the tendency of Tin to decrease with increasing air pressure value of the elastic element. This is because the increase in pressure should not affect the heat produced in the material of the flexible element and the heat produced by the

gas itself, according to numerical calculations, does not have a significant effect on the mean heat balance.

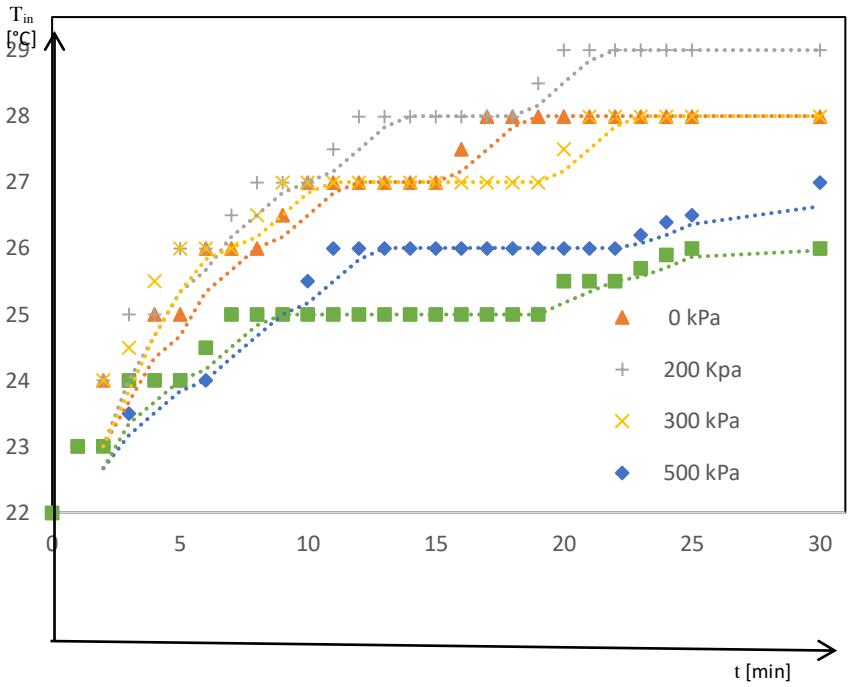

Fig. 6. The course of the temperature T_{in} at different pressures and speeds 800min^{-1}.

5 Conclusion

The article describes the change in temperature inside the elastic element when the pressure changes. In this article, we have described the flexible elements used in flexible shaft couplings developed at our department. We performed measurements on equipment developed in our laboratories and described its basic parts and described the movements it performs. We performed measurements at amplitudeA = 5.6 mm and three different speeds of 400, 600 and 800 min^{-1}. The aim of the article was to compare the effect of the temperature change of the inner shell of the elastic element at different pressures in the elastic element and therefore we performed measurements at different pressures. We also performed one measurement at a pressure of p = 0kPa, but this measurement did not show us any significant effects. Gradually, with increasing speed and increasing pressure, we noticed an important phenomenon. As the pressure in the elastic element increased, the temperature of the inner surface of the elastic element began to decrease. We noticed more significant changes at higher speeds. At a speed of n = 800min^{-1}, this process was better monitored than at a speed of n = 400min^{-1}.

This phenomenon occurs due to the admission of the fact that either the deformation energy or the proportion of heat loss on its value depends on the air pressure of the elastic element. This may be due to the fact that the material of the elastic element is permanently stressed by a high tensile stress and the polymer molecules of its rubber shell are all the more regularly arranged. With periodic deformations, such large losses of deformation energy do not occur and the proportion of losses decreases.

Another factor influencing the resulting temperature values is the rate of heat exchange between the gas and the rubber cord coating. This is significantly dependent on the gas pressure. When the pressure of the elastic element is higher, the heat dissipation rate is higher and therefore the resulting equilibrium temperature is lower. Both of these facts cause a surprising decrease in steady-state values of pressure temperatures.

Acknowledgments

This work was supported by the Slovak Research and Development Agency under the Contract no. APVV-19-0328.“
The article was written in the framework of Grant Projects:VEGA 1/0528/20, VEGA 1/0473/17, KEGA 006TUKE - 4/2020.

References

1. J. Homišin, P. Kaššay, M. Puškár, R. Grega, J. Krajňák, M. Urbanský, M. Moravič 2016 Continuous tuning of ship propulsion system by means of pneumatic tuner of torsional oscillation, International Journal of Maritime Engineering: Transactions of The Royal Institution of Naval Architects. 158, A3, A231-A238 (2016).
2. R. Grega, J. Krajnak J The pneumatic dual-mass flywheel, Scientific Journal of Silesian University of Technology - Series Transport 76 (2012).
3. J. Homišin Nové typy pružných hriadeľových spojok: vývoj, výskum, aplikácia. TU, SjF, Košice (2002).
4. J. Kostka, P. Frankovský, P. Čarák, V. Neumann Evaluation of residual stresses using optical methods. Acta Mechatronica. - Šemša (Slovensko), 4S go, 2016 Roč. 4, č. 4, s. 29-34 (2019).
5. G. Fedorko, P. Liptai, V. Molnár Proposal of the methodology for noise sources identification and analysis of continuous transport systems using an acoustic camera. Engineering Failure Analysis, 83, 30-46 (2018).
6. L. Jakubovičová, M. Sága, P. Kopas, M. Handrik M. Vaško Some Notes on Analysis of Bending and Torsion Combined Loading, Machine Dynamics Research 34, 3, 97–105 (2010).
7. L. Žuľová, R. Grega, J. Krajňák, G. Fedorko, V. Molnár Optimization of noisiness of mechanical system by using a pneumatic tuner during a failure of piston machine, Engineering Failure Analysis, 79, 845-851 (2017).
8. M. Puškár, M. Fabian, J. Kádárová, P. Blišťan, M. Kopas Autonomous vehicle with internal combustion drive based on the homogeneous charge compression ignition technology, In: International Journal of Advanced Robotic Systems, 14, 5, 1-8 (2017).
9. S. Maláková, F. Trebuňa, P. Frankovský Stress Analysis of Eccentric Gear with Asymmetrical Profile of Teeth 2016. American Journal of Mechanical Engineering, 4, 7, 390-393 (2016).

10. M. Moravec, P. Liptai Smart city concept system for the municipal waste disposal. International Journal of Interdisciplinarity in Theory and Practice, 12, 53-56 (2017).
11. M. Laciak, K. Kostúr, M. Durdán, J. Kačur, P. Flegner The analysis of the underground coal gasification in experimental equipment. Energy, 114, 332-343 (2016).
12. A. Sapietová, M. Sága, P. Novák Multi-software platform for solving of multibody systems synthesis, Communications 14, 3, 43– 48 (2012).
13. M. Saga, M. Vasko Stress Sensitivity Analysis of the Beam and Shell Finite Elements. Communications – Scientific Letters ofthe University Zilina, 11, 2, 5–12 (2009).
14. K. Kostúr, M. Laciak, M. Durdán Some influences of underground coal gasification on the environment. Sustainability, 10, 5, 1-31 (2018).
15. P. Czech, H. Madej Application of cepstrum and spectrum histograms of vibration engine body for setting up the clearance model of the piston-cylinder assembly for RBF neural classifier. Maintenance and Reliability, 4, 15-20 (2011).
16. G. Wojnar Model-based analysis of influence of coupling parameters on dynamic forces in gear meshing, Transactions of the Universities of Košice. Č. 3, s. 21-24 (2009).
17. M. Fabian, M. Puškár, R. Boslai, M. Kopas, S. Kender, R. Huňady Design of experimental vehicle specified for competition Shell Eco-marathon 2017 according to principles of car body digitisation based on views in 2D using the intuitive tool Imagine and Shape CATIA V5, Advances in Engineering Software, 115, 413-428 (2018).
18. P. Kaššay Effect of torsional vibration on woodchip size distribution. Scientific Journal of Silesian University of Technology. Series Transport, 99, 95-104 (2018).
19. M. Urbanský Comparison of piston and tangential pneumatic flexible shaft couplings in terms of high flexibility. Scientific Journal of Silesian University of Technology. Series Transport, 99, 193-203 (2018).
20. D. Harachová Decomposition of driving systems specified for rehabilitation machines, Ad Alta: Journal of Interdisciplinary Research, 7, 2, 271-273 (2017).
21. A. Mańka, A. Hełka J. Ćwiek Influence of copper content on pantograph contact strip material on maximum temperature of railroad wire. Scientific Journal of Silesian University of Technology. Series Transport, 2020, 106, 97-105 (2020).
22. A. Sapietová, M. Sága, I. Kuric et al. Application of optimization algorithms for robot systems designing. International Journal of Advanced Robotic Systems, 15, 1 (2018).
23. M. Sága, P. Kopas M. Uhričik Modeling and experimental analysis of the aluminium alloy fatigue damage in the case of bending - torsion loading. Procedia Engineering, 48, 599-606 (2012).
24. J. Kulka, M. Mantic, G. Fedorko, V. Molnar Failure analysis of increased rail wear of 200 tons foundry crane track. Eng. Fail. Anal., 67, 1–14 (2016).
25. P. Czech, G. Wojnar, R. Burdzik, L. Konieczny, J. Warczek Application of the discrete wavelet transform and probabilistic neural networks in IC engine fault diagnostics. J. Vibroengineering, 16, 1619 (2014).
26. L. Jakubovičová, M. Sága, M. Vaško M 2013 Impact analysis of mutual rotation of roller bearing rings on the process of contact stresses in rolling elements. Manuf. Technol., 13, 50–54 (2013).
27. J. Homisin et al. Removal of systematic failure of belt conveyor drive by reducing vibrations. In: Engineering Failure Analysis, 99 (2019).
28. H. Rahnejat Multi-body Dynamics: Vehicles, Machines and Mechanisms, Professional Engineering Publishing, Bury St Edmunds, UK (1998).
29. A. Wedin Reduction of Vibrations in Engines using Centrifugal Pendulum Vibration Absorbers, Chalmers University of Technology (2011).